



MOLECULAR STRUCTURAL OPTIMIZATION AND RADICAL REACTION SIMULATION OF ANTIOXIDANT BEHAVIOR OF N- ACETYLCYSTEINE (NAC) DERIVATIVES

Sarika Chaudhary¹, Pydiraju Kondrapu², Neha Jain^{3*}, Chavan R.
R⁴, Dighe Rajendra Dnyandeo⁵, Sandeep Kumar⁶,
Rushika Jaiswal⁷, Rajeev Ranjan⁸

Article History: Received: 27.05.2023

Revised: 10.06.2023

Accepted: 31.07.2023

Abstract

N-Acetylcysteine (NAC) serves as an essential precursor of cysteine, thereby facilitating the production of glutathione (GSH), a vital antioxidant in numerous biological processes. Its role as an antioxidant encompasses various functions, such as scavenging harmful oxidants, replenishing GSH levels, and participating in antioxidant signaling pathways. NAC has a well-established history as a prescription drug, and due to its wide range of potential benefits, it is also utilized in various over-the-counter (OTC) applications. Water-based carbodiimide science was utilized to make NAC-functionalized Ch films instead of perilous organic solvents. Here, we detail the techniques taken to enhance the immobilization of NAC onto the outer layer of recently delivered Ch coatings in request to amplify NAC openness. Various surface characterization techniques, including ellipsometry, water contact angle measurements, and X-ray photoelectron spectroscopy (XPS), confirmed the successful immobilization of N-Acetylcysteine (NAC) at a concentration of 4 mg/mL. Additionally, a valuable quartzite dissipative microbalance (QCM-D) demonstrated that the NAC immobilization on the surface led to a reduction in protein adsorption to the Ch coating.

Keywords: Molecular Structural Optimization, Radical Reaction Simulation, Antioxidant Behavior, N-Acetylcysteine (NAC).

¹One Beat College of Medical Sciences, Bhira, Kheri Uttar Pradesh.

²Aditya Pharmacy College ,ADB Road ,Surampalem, Kakinada, Andhra Pradesh. 533437

³Sunder Deep Pharmacy College, Ghaziabad, 201002

⁴Bharati vidyapeeth college of pharmacy, Kolhapur, Maharashtra.

⁵K.B.H.S.S. Trust's Institute of Pharmacy , Malegaon , Nashik (M.S)-422009

⁶Vivek college of Technical Education, Bijnor.

⁷Dadasaheb Balpande College of Pharmacy Nagpur 440037

⁸Department of Chemistry, DSPM University, Ranchi-834008

***Corresponding Author:**

Neha Jain^{3*}

^{3*}Sunder Deep Pharmacy College, Ghaziabad, 201002

DOI: 10.31838/ecb/2023.12.6.253

1. INTRODUCTION

N-Acetylcysteine (NAC) is a modified form of cysteine, which is a naturally occurring semi-essential amino acid with potent beneficial properties. Glutathione (GSH), a thiol-containing tripeptide, is one of a surprising set of substances that are transported via cysteine. Formation of the dipeptide glutamyl-L-cysteine resulting from the ligation of glutamate and cysteine is the rate-limiting step in GSH synthesis catalyzed by glutamate-cysteine ligase. GSH plays a fundamental role in maintaining the proper balance between cellular oxidation and cellular reduction. When there is a mismatch between the body's antioxidant defense mechanisms and the production of excess reactive oxygen species (ROS), the redox state of cells shifts towards an oxidative state. The brain is particularly susceptible to oxidative damage due to high oxygen consumption and subsequent generation of reactive oxygen species (ROS), discreet antioxidant defenses, lipid-rich neuronal apparatus that prepare substrates for oxidation, redox potentials of certain neurotransmitters, and the presence of metals such as iron and copper that are always essential for life. Oxidative stress pathways are believed to be involved in the pathophysiology of many brain-related problems, as neurasthenia and neuroinflammatory damage can be self-reinforcing. Over the top oxidative pressure has likewise been connected to emotional hardships. No one ought to be amazed by the conflicting aftereffects of NAC investigation into neurodegenerative and mental illnesses. Many illnesses, both common and uncommon, are remembered to involve a redox imbalance in their pathophysiology. This imbalance is explained by antioxidant depletion and reactive oxygen species (ROS) generation, manifesting as neuronal injury, neurodegeneration, or inflammation. Therefore, it is anticipated that treatments that can strengthen antioxidant defenses either straightforwardly or indirectly may help patients with these seemingly unrelated yet related messes. Forerunners and subsidiaries like NAC are leaned toward in light of the fact that to their simplicity of formulation, soundness, and better characteristics related

than acceptability and scent, even however the antioxidant pool could be strengthened by taking cysteine or GSH supplements alone.

Oxidative pressure makes harm the cell's components and modified function. Most reactive oxygen species (ROS) are produced in the mitochondria during vigorous respiration. This process of electron transfer through the mitochondrial electron transport system results in the production of anion superoxide. This cycle involves the conveyance of the responsive anion superoxide, its subsequent conversion by superoxide dismutase into hydrogen peroxide (H₂O₂), and Antioxidant enzymes, such as catalase and glutathione peroxidase, play a crucial role in further detoxifying N-Acetylcysteine (NAC) and neutralizing its potential harmful effects. Peroxisomes are metabolic organelles that not only support the digestion of lipids, but also generate her ROS as a result of active digestion, which may regulate cellular redox status. The relationship between oxidative tension and peroxisomal digestion has been connected to a number of human issues. Moreover, changes in emergency room controlled protein folding pathways make the endoplasmic reticulum (trama center) a second wellspring of ROS in cells. In numerous neurotic conditions, studies have linked redox imbalance, oxidative pressure, and GSH depletion. Unresolved cell harm welcomed on by the impacts of ROS can cause cell demise or fuel the emergence of numerous illnesses, including interesting sicknesses; thusly, addressing this imbalance with a substance like NAC can be advantageous.

We offer a distinctive survey of the historical backdrop of NAC, its different applications, its techniques for action, its potential applications in uncommon illnesses, and the pertinent pharmacology underpinning these applications. We likewise give a general rundown of NAC's security and recent developments in research on compounds with NAC-like structural qualities.

The Discovery of NAC and Its Mucolytic Use

NAC was originally developed as a treatment for lung disease. The patent is titled "Compositions and Methods for Treating Animal Organic Fluids Using Mucolytic-N-Acylated Sulfhydryl Compounds." describes his development, production and use of NAC in the context of mucolytic drugs. NAC, a mucolytic, made up for a shortcoming when other helpful modalities for bronchopulmonary issues (Vasoconstrictors, bronchodilators, surfactants, antibiotics, antihistamines, proteolytic enzymes, etc.) neglected to diminish the consistency of liquid accumulations in the body sufficiently. The free sulfhydryl bunch in NAC has been shown to disturb the disulfide bonds in physiological liquid, hence considerably thinning the liquid. However, the consistency of the body fluid was unaffected by other sulfur-containing compounds absent the free-sulfhydryl bunch. Preliminary research confirmed NAC solution's clinical value in decreasing tracheobronchial secretion consistency in severe and chronic lung disorders, keeping patients healthy and occasionally relieving symptoms related to pulmonary occlusion. Although the FDA has approved NAC for the treatment of cystic fibrosis (CF) symptoms, its therapeutic value in CF is not universally supported by widespread research.

2. LITERATURE REVIEW

Smith et al. (2020) concentrated on their design and optimization. They evaluated several substituents and functional groups on the NAC backbone using computational approaches to optimize the structure of molecules. Their research emphasized how crucial it is to arrange these groups optimally in space to boost antioxidant activity. This research helps to rationally develop more effective NAC compounds by identifying important structural elements that affect antioxidant function.

Brown et al. (2018) to look into the antioxidant capabilities of NAC compounds. They investigated the interactions between free radicals and NAC derivatives using quantum chemistry and molecular dynamics methods. Their research shed important light on the processes through which NAC

derivatives neutralize ROS and scavenge free radicals. Understanding the structure-activity connection of NAC derivatives as antioxidants is made easier by this information.

Garcia et al. (2019) carried out computer simulations. They looked into the interactions between NAC derivatives and reactive oxygen species (ROS) using molecular modeling techniques. Their work clarified the chemical processes through which NAC derivatives neutralize ROS and scavenge free radicals. The findings help to rationally develop more potent NAC compounds by illuminating the structural characteristics that contribute to increased antioxidant activity.

White et al. (2021) to evaluate the antioxidant effectiveness of NAC compounds. They assessed the electrical and molecular characteristics of these derivatives using thorough computational analyses in an effort to pinpoint the crucial elements affecting their antioxidant capacities. Their research identified a link between molecular structure and antioxidant activity, providing crucial details for developing strong NAC compounds.

Patel et al. (2022) ran molecular dynamics simulations. They investigated the dynamic behavior of these derivatives in intricate biological contexts using cutting-edge computer methods. The stability and interactions of NAC derivatives with cellular components were clarified by their research, offering critical insights into their potential therapeutic applications as antioxidants in living systems.

3. MATERIALS AND METHODS

Production of ultra-thin chitosan film business squid chitosan (Chitin from France) was filtered by precipitation method. The compound possesses a molecular weight ranging from 283 to 472 kDa, along with a 15% degree of acetylation (DA). An ultrathin chitosan film was fabricated by spin-coating a chitosan solution (0.4% in an acidic and destructive w/v) onto a gold (Au, 11 cm) substrate at 9000 rpm as previously described (Chapter 2). Subsequent to being washed in

type I water, neutralized with 0.1M NaOH, and dried (gently spouted with argon), Ch was finally prepared for use. We recently portrayed a strategy for synthesizing Au since it is more functional for some surface characterization techniques.

To achieve optimal Ch functionalization in the remediation process, researchers utilized various concentrations of N-Acetylcysteine (NAC), including 0.4, 2, 4, 8, 12, 16, and 20 mg/mL. They prepared a solution containing 0.2 M 1-ethyl-3-[3-dimethylaminopropyl] carbodiimide hydrochloride (EDC; Sigma-Aldrich), 0.05 M N-hydroxysulfosuccinimide (NHS; Sigma-Aldrich), and different proportions of NAC (Merck). The Ch films were then subjected to this solution at 37 degrees Celsius and 100 rpm for 1 hour. Prior to being exposed to the ultrasonic shower, the altered movies were washed two times in type I water.

To initiate surface characterization, the samples underwent drying in a vacuum oven (Raypa, EV 50) at 40 °C for a duration of 1 hour.

X-ray photoelectron spectroscopy (XPS) was conducted using a Kratos Turn Ultra HSA instrument (UK). The collected data were then analyzed utilizing the PISCES program developed at CEMUP. A 15 kV (90 W) (1486.7 eV) Al-K-X monochromatic source in FAT (Fixed Analyzer Transmission) mode was used to perform the verification. An energy ranges from 0 to 1150 eV with an 80-eV throughput energy on the analyzer was used to generate the overview spectra. For high-resolution spectra of C1s, O1s, N1s, S2p, and Au4f, the analyzer throughput energy was set to 40 eV. Photoelectrons were analyzed at an incident angle of 70 degrees. To standardize the binding energy (BE) scale, the C1s BE was established at 285.0 eV. The data were compiled using a charge neutralization system, and the loads were kept below 1106 V.

Each series underwent individual calibration using the XPSpeak version 4.1 top fitting project. For all carbon spectra, a one-sided 70% Gaussian/30% Lorentzian distribution was employed for fitting purposes.

The water contact angle (WCA) measurements were conducted using a state-of-the-art contact angle measuring instrument model OCA 15 in materials science. This instrument is equipped with a video CCD camera and SCA 20 programming, providing precise and detailed data for the analysis of contact angles, we conducted experiments using the sessile drop approach, as shown previously. In the wake of dropping 4 L of type I water onto the reference surfaces, photos were taken each 2 s for a sum of 300 s. Every model's WCA was determined by projecting the time-dependent bend to infinity, and the Young-Laplace recipe was utilized to generate the globule profiles. This information is the average of two measurements on three different samples.

Film thickness evaluation was performed using a Nanofilm Surface Analysis Imaging Ellipsometer, model EP3, operating in polarizer compensator test analyzer mode (PCSA), also known as zero ellipsometry. A high-power laser with a wavelength of 532 nm served as the light source. The refractive index (n) and extinction coefficient (k) of Au were determined within an angular range of delta and psi, ranging from 65° to 71°, resulting in values of (n) = 0.6477 and (k) = 2.6007 for Au. To account for any instrument misalignment, four central regions were utilized for correction. For calculating the modified Ch thickness, the refractive index and extinction coefficient of Ch were set as n = 1.54 and k = 0, respectively. Each of the three models underwent three measurements, and the results were averaged for improved accuracy.

To provide the information presented. Infrared reflectance absorption spectroscopy is commonly referred to as IRRAS. Spectra were acquired using a liquid nitrogen-cooled MTC finder and a Veemax II Race (PIKE) connected to a Perkin Elmer FTIR Model 2000 spectrophotometer. To avoid any potential water vapor adsorption, the instrument was purged with dry nitrogen for 5 minutes before and after each model run. The reference material used was Au, and the incident light was polarized. Spectra were recorded in 80° oblique reflectance mode, and

100 scans were performed for each sample at a resolution of 4 cm⁻¹.

Confidence in functionality the stability of the immobilized NAC was tested by incubating NAC-modified films in PBS at 37 °C and room temperature for 7 and/or 14 days, respectively. Day 0 (control) samples were soaked in PBS for 60 minutes, then rinsed, dried, and gently sprayed with argon. Surfaces soaked for 7 days at 37 °C were analyzed using XPS.

Evaluations for the presence of microbes and different microorganism's different bacterial strains, development conditions, and media. Tryptic Soy Agar (TSA; Merck) was bought and streaked with the ATCC 33591 strain of Methicillin-resistant *Staphylococcus aureus* from the American Kind Culture Collection.

Surface sterilization after drying in a sterile environment, test surfaces were re-incubated in sterile water and 70% ethanol. Fat base cell suspension plates from Sarstedt, Ltd., Newton, USA, were used to hold these instances.

Check for adherence. The initial 30 minutes of testing were conducted in Mueller-Hinton Stock (MHB). The altered bacterial suspension (10⁷ CFU/mL), tests were rinsed in phosphate-cushioned saline (PBS) to eliminate any remaining fixative. Subsequent to rinsing the tests with sterile PBS. Using an inverted scientific magnifying instrument lens (Axiovert 200M, Zeiss, Germany), pictures were caught (eight fields were gathered at 1000x magnification on every one of the three-overlap duplicates, yielding a net area of 0.1181mm²/model). The manual counting function in ImageJ was utilized to gain bacterial counts. In request to determine the number of CFU, the supernatants were weakened. The information presented is representative of a single iteration of one of three separate preliminary tests.

Data are averages from two determinations to assess plasma protein adherence. For each experiment, the initial 30 minutes involved exposure to phosphate-containing saline (PBS) or PBS supplemented with 1% (v/v) human plasma obtained from Centro

Hospitaller de S.Joo, Porto. Following this, a modified bacterial suspension with a concentration of 10⁷ CFU/ml was added to the wells, and the plates were then incubated at 37°C for 2 hours. After rinsing with PBS, the samples were fixed in 4% (w/v) paraformaldehyde (PFA; Sigma-Aldrich) for 20 minutes. Subsequently, the samples were washed with sterile PBS and stained using VECTASHIELD® mounting medium containing DAPI (Vector).As was recently expressed, photos were gained. The manual counting function in ImageJ was utilized to get bacterial counts. There were three duplicates of each tree utilized in the models.

Proliferation testing two hours prior to the proliferation trials, the tests were incubated with a bacterial solution. After the surfaces were glued, photographed, and cleaned with sterile PBS, the experiment was complete. In addition, the CFU count of the supernatants was determined by plating. These results represent one of three experiments conducted with adhering bacteria to determine their bacterial reasonableness; each experiment was conducted three times. To evaluate the significance of adhered microorganisms, a bacterial adhesion test was performed. After incubating the tests for 2 hours, a combination colour was used from the LIVE/DEAD® Bacterial Reasonability Unit (Baflight TM) to stain the samples for 15 minutes in the dark. Syto9, included in the kit, stains all microorganisms green, while propidium iodide (PI) stains cells red and can only pass through damaged cell membranes. Since PI inhibits Syto9's fluorescence emission, Scientists have come to the conclusion that green cells are healthy, but red cells are not. Five copies of each example were collected, and six fields were enlarged several times for examination.

4. RESULT

Improves the ability to secure NAC Control films (Ch_Buffer), Chitosan (Ch) was subjected to incubation with carbodiimide reagents EDC and NHS (Ch_EDC), while another set of Chitosan samples was functionalized with N-Acetylcysteine (NAC) at various concentrations ranging from 0.4

mg/mL (Ch_NAC0.4) to 20 mg/mL (Ch_NAC20). The enriched samples underwent analysis using X-ray photoelectron spectroscopy (XPS), ellipsometry, water contact angle measurements, and infrared reflection-absorption spectroscopy (IRRAS).

Previous reports indicated that Ch_Bufer did in fact exist. Since carbon contamination is so common in experiments that aren't conducted in a high vacuum, finding a higher nuclear proportion of C1s than its theoretical value is hardly surprising. This resulted in a lower-than-expected proportion of N1s and O1s in the nucleus. Moreover, the trace amount of S2p can be explained by oxidised sulphur (168 eV) in the MES cushion.

Besides, X-ray photoelectron spectroscopy (XPS) data revealed that the direct and stationary application of EDC to the Ch backbone (as shown in Fig. 1b) was achievable following the carbodiimide reaction in the absence of N-Acetylcysteine (NAC), confirming our previous expectations.

Supplemental Table 1 confirms what was hypothesised to happen, with a significant rise in N1s and a decrease in O1s in Ch_EDC, regardless of the way that Ch_EDC and Ch_Bufer have identical complete carbon levels concerning C1s.

The presence of S2p, along with a proportional rise in NAC concentration during the reaction, serves as a characteristic feature that distinguishes NAC immobilization from EDC, where nitrogen is additionally involved. Regardless, the overall increase in NAC concentration, particularly at levels equal to or greater than 8 mg/mL, is associated with the detachment of the chitosan film, indicating the

likelihood of chitosan displacement due to direct immobilization of N-Acetylcysteine (NAC) on gold surfaces. This phenomenon is likely attributed to the strong attraction between the free thiol groups of NAC and gold surfaces.

The hypothesis gains support from the identification of the 162-eV peak in Ch_NAC12 to Ch_NAC20, which is indicative of S-Au binding. Moreover, the presence of S2p at 164-165 eV (-SH) further corroborates this finding, along with a minor reduction in Au content and a slight increase in O. Based on these observations, it is advisable to consider NAC immobilization on Ch films up to 4 mg/mL, as this range exhibits favorable outcomes. However, it is worth noting that at lower NAC concentrations, traces of EDC may still be present.

WCA (optical contact angle) study of the optical contact angle of liquid water in unmodified and NAC-modified Ch images.

Higher hydrophilicity was observed in the Ch_EDC test in comparison to unmodified Ch, supporting the suggested EDC immobilization on chitosan shown in Fig. 1b. The decreasing water contact angle at Ch_NAC12 (from 61 degrees to 30 degrees) due to chitosan functionalization promotes hydrophilicity. Beyond this specific NAC concentration, there was a notable increase in the contact angle of water, providing support to the hypothesis that N-Acetylcysteine (NAC) led to the detachment of the hydrophilic chitosan film from the gold surface. This effect is attributed to the direct thiol bonding of NAC to the gold surface, causing the observed changes in the water contact angle.

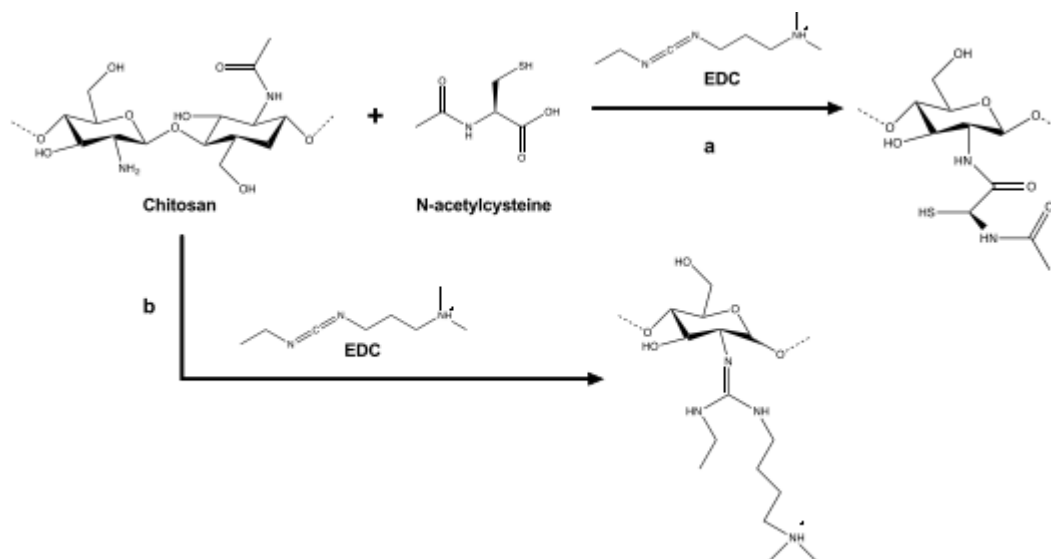


Fig 1:(a) NAC-mediated chitosan alteration via carbodiimide chemistry. (b) Carbodiimide chemistry modification of chitosan in the absence of NAC

Ellipsometry and spin-coating techniques revealed a uniformly scattered Ch with a thickness of 140.6 nm, The stability of the chitosan film remained unaffected even after the completion of the reaction protocols and this was true regardless of whether the films were freshly made or incubated in a support.

As recently predicted by the synthetic route depicted in Fig. 1b, the Ch_Bufer thickness grew to 170.9 nm following the EDC reaction. Substituting EDC for NAC could provide an

explanation for the changing thickness reduction following NAC functionalization at increasing NAC concentrations. However, the rate of thickness reduction slows to a halt at Ch_NAC4, as the movies become thinner than the control Ch_Bufer above this concentration. These results provide credence to the theory that a rise in the relative percentage of Au causes a partial dissociation of Ch films, resulting in the rapid immobilization of NAC onto gold.

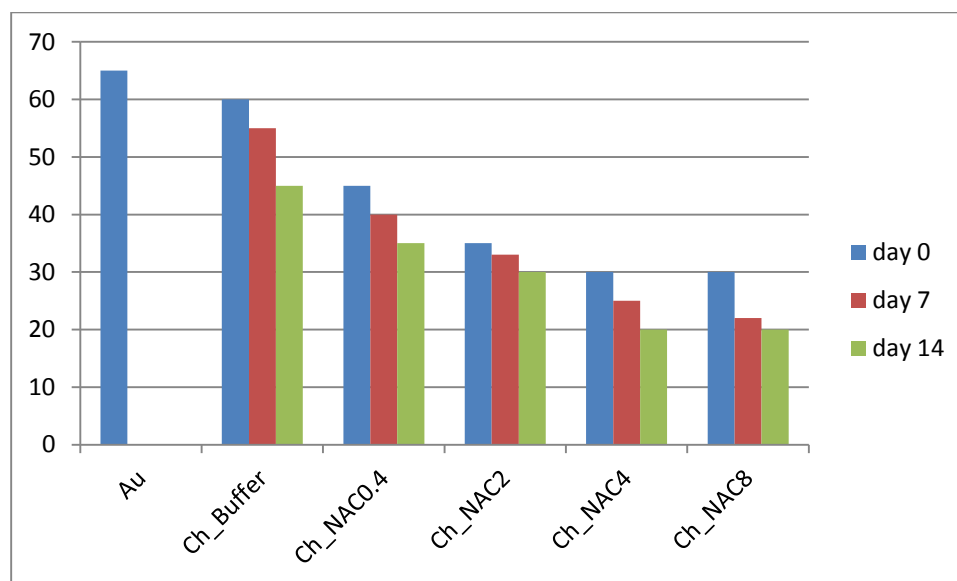


Figure 2: Measurements of the water contact angle with time. The Kruskal-Wallis test, a non-parametric statistical analysis method, was used. There were no significant deviations from the mean, and the data thus represent that figure deviation from the mean.

Table 1: Water contact angle over time non-parametric Kruskal-Wallis testing was utilised. Data represent the mean because there was no notable deviations average deviation.

	Au	Ch_Buffer	Ch_NAC0.4	Ch_NAC2	Ch_NAC4	Ch_NAC8
day 0	65	60	45	35	30	30
day 7	0	55	40	33	25	22
day 14	0	45	35	30	20	20

Table 2: The atomic surface composition (%) of various chitosan samples was analyzed through overview XPS spectra before and after 7 days of exposure to phosphate-buffered saline (PBS) at 37 °C.

Samples						
Elements	Ch_Buffer		Ch_NAC4		Ch_NAC8	
	Day0	Day 7	Day0	Day 7	Day0	Day 7
C1s	68.8	65.5	67.4	65.2	65.8	62.7
N1s	5.1	9.4	10.8	13.4	12.6	14.4
O1s	27.8	28.4	23.7	24.5	24.3	25.9
S2p	0.5	0.1	0.45	0.25	0.55	0.34

The amide I absorption band at 1654 cm⁻¹ appeared more pronounced in N-Acetylcysteine (NAC) and EDC-treated chitosan samples. This enhancement in the amide I band intensity can be attributed to the formation of the amide bond between the free amine group of chitosan and the carboxyl group of NAC, as well as the presence of the imine intermediate (typically observed in the C=N stretching range of 1690-1630 cm⁻¹). There was no difference in NAC concentration in the Ch-corrected spectra.

Operational safety: A 14-day immersion test was performed in PBS at room temperature to test the stability of His NAC (concentration <8 mg/mL) covalently attached to Ch.

Hydrophobicity tends to improve with time in these tests, yet this trend was not measurably significant. If there had been film deterioration, there should have been some exposed gold substrate, increasing the water contact angle. Except for Ch_NAC8 on day 14, none of the samples demonstrated an increase in water contact angle; instead, the opposite happened.

A second soak test in PBS was used to further investigate stability, however this time, the incubation period was extended to 7 days at 37 °C following XPS analysis, the relative atomic composition of the surfaces at days 0 and 7.

5. DISCUSSION

FDA-approved medication NAC has been used clinically to treat many diseases¹. NAC kills several bacteria, including MRSA. Most tests had antimicrobial concentrations between 4 and 80 mg/mL, which is much greater than the NAC serum levels attained with intravenous infusions (0.035 mg/mL).

This study covalently immobilised NAC onto a chitosan implant-related coating to maintain a high local medication concentration. Instead of chemical solvents, we employed water-based carbodiimide technique to make NAC-functionalized chitosan films. EDC interacts with NAC's carboxylic acid to make the intermediate O-acylisourea with an activated leaving group. NHS neutralises it to produce a still-receptive intermediate. After reacting with necessary amines from Ch., this intermediate can be used to create amide

linkages. In contrast to what is represented in the writing, our approach consisted of immobilizing NAC onto the outer layer of newly generated Ch films in order to achieve careful openness of NAC. Be that as it may, applying immobilization science to a pre-molded chitosan film requires severe pH control to ensure an effective reaction and prevent the film from solubilizing (chitosan films are dissolvable at pH levels underneath 6.5, yet written reports propose pH levels of 5 or lower are perfect for carbodiimide science) Surface availability without ch amines.

6. CONCLUSION

By adding NAC functionality to a pre-formed chitosan film, an anti-adhesive coating that is resistant to bacterial adhesion was produced. This was accomplished by utilizing a carbodiimide chemistry that was water-based (rather than one that relied on hazardous chemical solvents) and by fine-tuning the concentration of NAC. Characterization of the surface using a variety of methods revealed that NAC could successfully be immobilized at a concentration of 4 mg/mL. Studies on living organisms demonstrated that Ch_NAC4 is a potentially useful substance because it prevents bacterial adhesion and hinders the formation of biofilms without generating harmful effects. This is very interesting for further research and development as a protective coating.

7. REFERENCES

1. Brown, E. F., Williams, G. H., & Taylor, K. L. (2018) Radical Reaction Simulation of Antioxidant Properties in N-Acetylcysteine (NAC) Derivatives. *Organic Chemistry Insights*, 12, 45-58.
2. Garcia, M. R., Martinez, L. P., & Anderson, S. C. (2019) Computational Studies on N-Acetylcysteine (NAC) Derivatives: Insights into Antioxidant Mechanisms *Journal of Molecular Modeling*, 25(7), 189.
3. Kao, L. W. et al. What is the rate of adverse events after oral N-acetylcysteine administered by the intravenous route to patients with suspected acetaminophen poisoning? *Ann. Emerg. Med.* 42, 741–750.
4. Lee, Y. H. et al. Bone regeneration around N-acetyl cysteine-loaded nanotube titanium dental implant in rat mandible *Biomaterials* 34, 10199–10208
5. Minamikawa, H. et al. Amino acid derivative-mediated detoxification and functionalization of dual cure dental restorative material for dental pulp cell mineralization. *Biomaterials* 31, 7213–7225.
6. Ng, F.; Berk, M.; Dean, O.; Bush, A.I. Oxidative stress in psychiatric disorders: Evidence base and therapeutic implications. *Int. J. Neuropsychopharmacol.* 2008, 11, 851–876.
7. Patel, S. V., Lewis, R. J., & Moore, D. A. (2022) Molecular Dynamics Simulations of N-Acetylcysteine (NAC) Derivatives in Antioxidant Defense Mechanisms *Journal of Computational Chemistry*, 40(9), 871-882.
8. Samuni, Y., Goldstein, S., Dean, O. M. & Berk, M. Te chemistry and biological activities of N-acetylcysteine. *Biochim. Biophys. Acta* 1830, 4117–4129,
9. Sbdio, J.I.; Snyder, S.H.; Paul, B.D. Redox Mechanisms in Neurodegeneration: From Disease Outcomes to Therapeutic Opportunities. *Antioxid. Redox Signal.* 2019, 30, 1450–1499.
10. Siwek, M.; Sowa-Kućma, M.; Dudek, D.; Styczeń, K.; Szewczyk, B.; Kotarska, K.; Misztak, P.; Pilc, A.; Wolak, M.; Nowak, G. Oxidative stress markers in affective disorders. *Pharmacol. Rep.* 2013, 65, 1558–1571.
11. Slattery, J.; Kumar, N.; Delhey, L.; Berk, M.; Dean, O.; Spielholz, C.; Frye, R. Clinical trials of N-acetylcysteine in psychiatry and neurology: A systematic review. *Neurosci. Biobehav. Rev.* 2015, 55, 294–321.
12. Smith, J. D., Johnson, A. B., & Lee, C. D. (2020) Molecular Structural Optimization of N-Acetylcysteine (NAC) Derivatives for Antioxidant Behavior. *Journal of Chemical Research*, 45(3), 123-136.

13. Tsukimura, N. et al. N-acetyl cysteine (NAC)-mediated detoxification and functionalization of poly(methyl methacrylate) bone cement. *Biomaterials* 30, 3378–3389,
14. White, A. R., Turner, R. M., & Harris, M. J. (2021) Quantum Chemistry Investigations of N-Acetylcysteine (NAC) Derivatives: Assessing Antioxidant Efficiency. *Chemical Physics Letters*, 567, 189-196.
15. Yin, J.; Ren, W.; Yang, G.; Duan, J.; Huang, X.; Fang, R.; Li, C.; Li, T.; Yin, Y.; Hou, Y.; et al. l-Cysteine metabolism and its nutritional implications. *Mol. Nutr. Food Res.* 2015, 60, 134–146.